Ecotoxicology and Environmental Safety 283 (2024) 116795

Contents lists available at ScienceDirect

Ecotoxicology and Environmental Safety

journal homepage: www.elsevier.com/locate/ecoenv

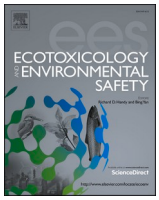

The occurrence of positive selection on BicA transporter of *Microcystis aeruginosa*

Eun-Jeong Kim, Huijeong Doh, Jihye Yang, Seong-il Eyun *

Department of Life Science, Chung-Ang University, Seoul 06974, Korea

ARTICLE INFO

Edited by Professor Bing Yan

Keywords:
BicA transport
Positive selection
CCMs
Microcystis aeruginosa
PAML

ABSTRACT

The rapid growth of cyanobacteria, particularly *Microcystis aeruginosa*, poses a significant threat to global water security. The proliferation of toxic *Microcystis aeruginosa* raises concerns due to its potential harm to human health and socioeconomic impacts. Dense blooms contribute to spatiotemporal inorganic carbon depletion, promoting interest in the roles of carbon-concentrating mechanisms (CCMs) for competitive carbon uptake. Despite the importance of HCO_3^- transporters, genetic evaluations and functional predictions in *M. aeruginosa* remain insufficient. In this study, we explored the diversity of HCO_3^- transporters in the genomes of 46 strains of *M. aeruginosa*, assessing positive selection for each. Intriguingly, although the *Microcystis* BicA transporter became a partial gene in 23 out of 46 genomic strains, we observed significant positive sites. Structural analyses, including predicted 2D and 3D models, confirmed the structural conservation of the *Microcystis* BicA transporter. Our findings suggest that the *Microcystis* BicA transport likely plays a crucial role in competitive carbon uptake, emphasizing its ecological significance. The ecological function of the *Microcystis* BicA transport in competitive growth during cyanobacterial blooms raises important questions. Future studies require experimental confirmation to better understand the role of the *Microcysits* BicA transporter in cyanobacterial blooms dynamics.

1. Introduction

Harmful cyanobacterial blooms pose a major threat to freshwater ecosystems, causing widespread economic damage worldwide (Wang et al., 2023; Yuan et al., 2019). For instance, increased phosphorus loading in Lake Erie has led to the recurrence of harmful algal blooms, potentially costing Canada $5.3 billion over the next 30 years if not managed (Smith et al., 2019). During the summer, elevated temperatures and intense light levels facilitate a surge in photosynthesis, allowing cyanobacteria to exponentially increase their population and form blooms (Berry et al., 2017; Griffith and Gobler, 2020). For photosynthesis, cyanobacteria utilize inorganic carbon (Ci) present in lakes to fix CO_2 within cells (Ji et al., 2020; Kupriyanova et al., 2013). To accumulate CO_2 efficiently, cyanobacteria have evolved carbon-concentrating mechanisms (CCMs), allowing them to achieve up to 1000-fold concentrations of CO_2 around RuBisCo compared to the extracellular environment (Raven et al., 2012; Reinhold, 1999). However, spatiotemporal depletion of dissolved CO_2 concentrations occurs in eutrophic lakes when cyanobacterium *Microcystis aeruginosa* thrives. At this stage, CCMs may confer a competitive advantage for the uptake of Ci.

The effects of cyanobacterial CCMs on photosynthetic efficiency have been extensively investigated in the model species such as *Synechococcus* PCC7942 and *Synechocystis* PCC6803 (Price et al., 2004; Shibata et al., 2002). These studies revealed that gene associated with CCMs are closely correlated with the depletion of the internal Ci pool. On the other hand, as a recent concern, CCMs may play a crucial role as a selection factor in cyanobacterial blooms, particularly in response to the rising atmospheric CO_2 levels (Ji et al., 2020). Furthermore, both field data and experiments have demonstrated the selection strength of specific Ci transporters, underscoring their eco-physiological importance. In freshwater, *M. aeruginosa* is a blooming cyanobacterium that produces the hepatotoxin microcystin (MC), causing economic losses by diminishing water quality in lakes and brackish waters (Berry et al., 2017; Dick et al., 2021; Tanabe et al., 2018). However, evidence of the involvement of Ci uptake systems in the exponential population increase of *Microcystis* is insufficient, despite the ecological and social issues it causes.

The Ci uptake systems of cyanobacteria deliver CO_2 and HCO_3^- into cells as a source of carbon. There are five modes of cyanobacterial Ci

* Corresponding author.
E-mail address: eyun@cau.ac.kr (S.-i. Eyun).

https://doi.org/10.1016/j.ecoenv.2024.116795
Received 19 March 2024; Received in revised form 10 July 2024; Accepted 24 July 2024

uptake systems, with two being CO_2 uptake systems (NDH-1_3 and NDH-1_4), located on the thylakoid. The other three, HCO_3^- transporters (BicA, SbtA, and BCT1), are located on the cytoplasmic membrane (Gaudana et al., 2015). HCO_3^- transporters directly accumulate external HCO_3^- inside the cell, while CO_2 diffused into cells undergoes a conversion process to HCO_3^- facilitated by specialized NDH-1 complexes in the thylakoid membrane. Eventually, only HCO_3^- can diffused into carboxysomes, where carbonic anhydrase converts HCO_3^- to CO_2 in close proximity to Rubisco (Battchikova et al., 2010). Interestingly, intracellular CO_2 is converted to HCO_3^- on the thylakoid membrane, whereas HCO_3^- bypasses the thylakoid membrane and directly enters the carboxysome. These studies indicate that various cyanobacterial species possess different sets of bicarbonate transporters (SbtA, BCT1, and BicA) with varying affinities and capacities for bicarbonate uptake. In 17 well-described thermophilic cyanobacteria, comparative genomics revealed that all strains possessed two CO_2 uptake systems and BicA, whereas most strains lacked SbtA. Additionally, BCT1 was absent in only four strains (Tang et al., 2022). Some cyanobacteria have developed specialized CCMs to thrive in specific environmental conditions. For example, *Anabaena* sp. can form heterocyst to fix nitrogen and regulate CCMs for optimal carbon fixation in nitrogen-limited environments (Herrero and Flores, 2019). A bicA strain of *M. aeruginosa* adjusts its CCM activity in response to elevated pCO_2 in laboratory chemostats. However, caution is advised in interpreting these associations, as they were used only a few strains (Ji et al., 2020).

HCO_3^- transporters in cyanobacteria exhibit greater genetic diversity compared to CO_2 transporters, potentially providing an advantage in adapting to fluctuating Ci limits during *Microcystis* blooms. Speculatively, it is worth considering that the biological function of HCO_3^- transporters in early Ci uptake may be to enhance the accumulation of photosynthetic carbon under carbon limitation. BicA is one of the key bicarbonate transporters in cyanobacteria, characterized as a constitutively-expressed, high-flux, low-affinity Na^+/ HCO_3^- symporter ($K_m = 70–350$ μM) (Price, 2011). This belongs to the SulP/SLC26 family of transporters, which are found in both eukaryotes and prokaryotes (Rolland et al., 2016). During blooms, *Microcystis* bicA strain appear to be better adapted to high HCO_3^- conditions compared to three green microalgae (Ji et al., 2017). When bicarbonate levels are enriched in the field, *Microcystis* strains carrying bicA demonstrate dominance over those with bicA+sbtA during blooms. This research aims solely to explore the diversity of bicarbonate uptake genes (Sandrini et al., 2016). Therefore, our study focuses on the mechanisms of evolutionary adaptation in bicarbonate genes, particularly on transporters favored by natural selection, which remains largely unexplored.

Next-generation sequencing (NGS) technologies have offered new insights into the genome complexity and genetic diversity of *Microcystis aeruginosa* (Li et al., 2018; Okano et al., 2015). The genomic structures of *M. aeruginosa*, first published in 2008 with the NIES-843 strain, have been elucidated through NGS technologies (Kaneko et al., 2007). Since then, *M. aeruginosa* NIES-843 has served as a reference genome for assembling newly sequenced genomes. As of May 2023, a total of 154 genomes of *M. aeruginosa*, including metagenomic data have been submitted to the NCBI database. In this study, we first demonstrated that the defective bicA gene in *Microcystis* was randomly selected based on the synteny and phylogenetic analysis. Furthermore, we found strong statistical evidence of positive selection acting on the BicA transporter. The *in silico* analysis confirmed the substrate-binding sites on BicA and identified covalent links between the TM2 and TM8 regions, which form the substrate-binding pocket. These links potentially enhancing the structural stability, an idea that requires further verification. These results suggest that *Microcystis* BicA, as a HCO_3^- transporter, represents the most promise as an evolutionary adaption candidate for gene evolution and future ecogenetics studies.

2. Methods

2.1. Genome dataset

One hundred and fifty-four genomes of *Microcystis aeruginosa* are currently reported on the NCBI website (as of May 2023). In this study, we used complete or near-complete genomes, eliminating 108 metagenomic strains from a total of 154 genomes (Jeon et al., 2023; Jung et al., 2020). Ultimately, we obtained 46 single-strain genomes, which consisted of less than 814 contigs (Table S1). Table S1 shows the genomic information of all 46 strains, including six strains completely assembled into single scaffolds/contigs (*Ma*_NIES-843, _NIES-298, NIES-2549, _NIES-2481, _PCC 7806SL, and _FD4). The others consisted of a few scaffolds or numerous contigs.

2.2. Phylogenetic analysis

The basic local alignment search tool (BLAST) search identified the protein sequences of 20 housekeeping genes using the protein sequences of NIES-843 as the queries (Table S2). A BLAST E-value cutoff of less than 1.0×10^{-200} resulted in greater than 97 % sequence similarities. Phylogenetic analyses were based on the maximum-likelihood method with 4721 concatenated amino acid sequences of 20 housekeeping genes. Previous studies observed that toxic and non-toxic strains can be distinguished by multilocus sequence typing (MLST) or ribosomal proteins (Sun et al., 2016; Tanabe et al., 2007). In this study, we selected 6 MLST loci and 14 large (50 S) ribosomal proteins (LRPs). Toxic strains were genetically distinct from non-toxic strains in their MLST allelic profiles (Tanabe et al., 2007), the universal LRPs were conserved in Bacteria, Archaea, and Eukaryotes (Ban et al., 2014). The six MLST loci included cell division protein FtsZ (415 aa; BAG02464.1), glutamine synthetase GlnA (473 aa; BAG01749.1), glutamyl-tRNA synthetase GltX (480 aa; BAG05091.1), glucose-6-phosphate isomerase Pgi (524 aa; BAG04645.1), recombination protein RecA (355 aa; BAG01429.1), and triosephosphate isomerase Tpi (230 aa; BAG00951.1). The fourteen LRPs included L1 (237 aa; BAG03485.1), L2 (277 aa; BAG05562.1), L3 (212 aa; BAG05565.1), L4 (210 aa; BAG05564.1), L5 (179 aa; BAG05553.1), L10 (182 aa; BAG04209.1), L11 (141 aa; BAG03484.1), L13 (151 aa; BAG05073.1), L15 (147 aa; BAG05548.1), L16 (80 aa; BAG05558.1), L18 (120 aa; BAG05550.1), L22 (119 aa; BAG05560.1), L24 (117 aa; BAG05554.1), and L29 (72 aa; BAG05557.1). The multiple sequence alignments were performed in MAFFT (ver. 7.475) using the L-INS-i algorithm (Katoh and Standley, 2013). The phylogenetic tree was constructed in MEGA (ver. 11.0.13) (Tamura et al., 2021) and 1000 bootstrap replicates were performed to estimate the confidence levels of the branching topology. The tree is visualized with a midpoint root using FigTree (ver. 1.4.3) (http://tree.bio.ed.ac.uk/software/figtree).

2.3. The mining of the bicarbonate transporter genes and loci

A BLAST search identified the nucleotide sequences of three bicarbonate transporter genes. The protein sequences of NIES-843 were used as the queries except for in the case of the full bicA sequences of PCC 9806 due to NIES-843 only possessing partial bicA sequences (Harke and Gobler, 2015; Zhou et al., 2019). A BLAST e-value cutoff of less than 1.0×10^{-200} resulted in greater than 90 % sequence similarities. Using the BLAST results, we identified the genetic position of the bicA–sbtA and BCT1 operons, which are summarized in Table S3 and S4, respectively. The bicA–sbtA loci consists of ccmR2 (876 nt, RS27130), bicA (1701 nt, MICAE_1030025 for PCC9806), sbtA (1121 nt, RS27140), sbtB (338 nt, RS27145), and nhaS3 (1416 nt, RS27150). The BCT1 operon comprises ccmpA (1359 nt, RS08745), ccmpB (830 nt, RS08750), ccmpC (2019 nt, RS08755), and ccmpD (840 nt, RS087660). The above RS numbers are the locus tags of NIES-843.

2.4. Estimating d_N/d_S values and positively selection sites

Estimations of the non-synonymous and synonymous nucleotide substitutions and the detection of positive Darwinian selection in protein-coding DNA sequences were performed using codeml in PAML package (ver. 4.9 g) (Zhang et al., 2005). Codeml computes the posterior probability that a codon can be classified as influenced by positive selection. Several LRTs (likelihood ratio tests) were implemented to compare PAML site models and two had good power and low false-positive rates. This included three steps, each comparing two distinct models: first, the one-ratio model (M0) vs. the discrete model (M3); second, the neutral model (M1) vs. the selection model (M2); and third, the beta distribution (M7) vs. the alternative model (M8). Previous studies have presented each model in detail (Eyun, 2019).

Branch-site models were employed to detect positive selected amino acid sites that were identified based on Bayes Empirical Bayes (BEB) posterior probabilities. In these models, positive selection was allowed on a specific foreground branch and LRTs were conducted against null models that assumed no positive selection. All PAML analyses were carried out using the F3X4 model of codon frequency. The level of significance (p-value) for the LRTs was estimated using a χ^2 distribution with the given degrees of freedom. The test statistic was calculated as twice the difference of the log-likelihood between the models: $2\Delta lnL = 2(lnL_1 - lnL_0)$, where L_1 and L_0 are the likelihood of the alternative and null models, respectively.

2.5. Topology prediction

Several web-based programs were used to examine the BicA protein sequence and predict membrane topology. The CCTOP website (https://cctop.ttk.hu) was used to produce a consensus prediction of the Microcystis BicA transporter's membrane protein topology based on nine methods: HMMTOP, Memsat-SVM, Octopus, Philius, Phobius, Pro, Prodiv, Scampi, and TMHMM. The transmembrane topology was also predicted using MemBrain (ver. 3.1) (http://www.csbio.sjtu.edu.cn/bioinf/MemBrain). This result includes both *N* and *C* terminals located in the cytoplasm and 14 transmembrane helices. The topology of BicA transmembrane proteins was visualized using Protter (ver. 1.0; http://wlab.ethz.ch/protter).

2.6. 3D homology modeling

Homology-based structural modeling was performed using the SWISS-MODEL web server (https://swissmodel.expasy.org). Recently, the crystal structure of the *Synechocystis* PCC6803 BicA was determined (Wang et al., 2019) and *Synechocystis* BicA is phylogenetically close to *Microcystis* BicA (Price et al., 2011). Consequently, we used the 6ki1 structure from the SulP domain of the *Synechocystis* PCC6803 BicA transporter as the template, which exhibited 68.1 % protein identity with the *Microcystis* NIES-9807 BicA. The *Synechocystis* BicA protein was crystallized using a lipid cubic phase (LCP) system and the structure was determined at a resolution of 2.8 Å(Wang et al., 2019). A graphical representation of BicA structures was constructed using PyMOL (ver. 2.5) (https://pymol.org).

3. Results

3.1. The genomes of the Microcystis aeruginosa strains

We collected sequence read archive (SRA) data from the NCBI website for 46 strains of *M. aeruginosa* (https://www.ncbi.nlm.nih.gov/datasets/genome/?taxon=1126). All genomic information, including assembly/biosample accession numbers and geographic location, is summarized in Table S1. The 46 genomes averaged 4.9 Mbp in length, and the number of protein-coding genes ranged from 3531 to 5220. The whole-genome lengths of the 46 strains were proportional to the number of protein-coding genes they contained (Fig. S1a). Genome sizes ranged from 3.9 to 5.9 Mbp, and the number of protein-coding genes differed by 1631 genes between the smallest and largest genomes, which included 3531 and 5162 genes, respectively. The G+C contents of the 46 genomes ranged from 42.1 % to 43.5 % (Fig. S1b). The strains showed high genome size dynamics, primarily related to gene gains/losses, which were associated with the differences in protein-coding gene numbers. The G+C contents showed stability compared to the high genomic fluctuation. In this study, we focused on the bicarbonate transporters of the 46 genomic strains, which will serve as fundamental knowledge for studying the photosynthetic carbon accumulation and population growth of the bloom-forming cyanobacterium *M. aeruginosa*.

3.2. The diversity of bicarbonate transporters among 46 Microcystis strains

To determine the phylogenetic relationship of the 46 strains of *M. aeruginosa*, a phylogenetic tree was generated using the concatenated amino acid sequences of 6 housekeeping genes and 14 large ribosomal proteins, obtaining a long alignment of 4721 amino acids in total (Table S2). Previous studies showed that toxic and non-toxic strains formed distinct clades when using multilocus sequence typing (MLST) or ribosomal proteins (Sun et al., 2016; Tanabe et al., 2007). Thus, we selected 6 MLST loci (Tanabe et al., 2007) and 14 large (50 S) ribosomal proteins (LRPs) as marker genes for the phylogenetic analysis. Expectedly, the result showed two highly supported monophyletic clades, labeled Clades I and II (Fig. 1). All toxic strains fell into Clade I, which was further split into two subclades, a toxic and mixed group (groups A and B in Fig. 1). Note that Clade I and II showed bootstrap values below 50 %, with only Clade I group A having statistical support at 79 %. This midpoint-rooted phylogenetic tree inadequately represented evolutionary relationships. Interestingly, half of the 46 strains possessed partial bicA sequences (218–257 nt in size) at the 5′ end, and the other half had a full-length bicA gene (1700 nt in size). All non-toxic strains of Clade II contained the full-length sbtA gene (1120 nt in size), and thus none contained bicA gene alone. This phenomenon remained consistent in all non-toxic strains of group B. These results suggest that gene recombination in the HCO_3^- transporters has been common. Although genetic recombination occurs by chance, it seems worthwhile to investigate whether the recombination of HCO_3^- transporters affects biomass increases by promoting photosynthesis. Distinctively, four strains, all originating from Lake Kasumigura in Japan (Table S1), had an IS605 transposon insertion between the partial bicA gene and full-length sbtA. A previous study reported a similar feature in strains CCAP 1450/10 and 1450/11(Sandrini et al., 2014), but it is newly reported here in strains NIES-2521, 3787, 3804, and 3807 (identified by the shaded orange box in Fig. 1). In addition, a microcystin synthetase (mcy) gene cluster consisting of 10 genes (mcyA - J) responsible for producing hepatotoxin microcystins was blasted (MC in Fig. 1). In this study, there was no correlation found between HCO_3^- transporters and toxin-producing strains.

In summary, half of both toxic and non-toxic strains possessed the partial bicA and sbtA gene, a condition widely distributed in different continents (Fig. 1 and Table S1), indicating that a common ancestor may have lost most of its toxic genes and the full bicA gene first, then spread all over the world (Rantala et al., 2004). In terms of genetic diversity, the bicA–sbtA loci are more interesting than the BCT1 operon because the BCT1 gene is significantly conserved across all strains (Fig. 1). Next, we intensively surveyed the genomic position of the bicA and sbtA genes using the genome sequences.

3.3. The loci of the bicA–sbtA genes

To investigate genetic rearrangement in the bicA–sbtA loci, we identified co-localization using two neighboring genes. The upstream

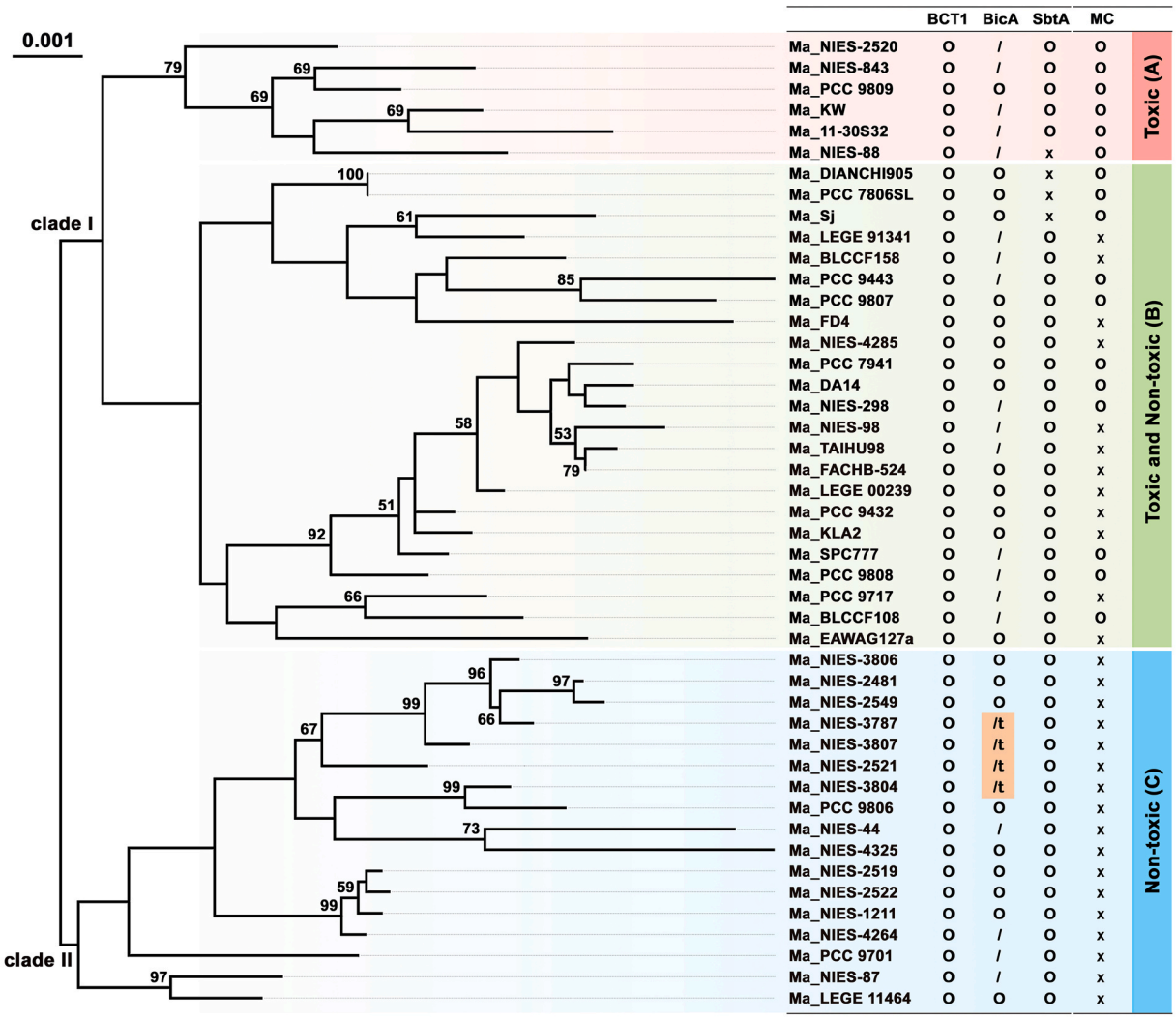

Fig. 1. Maximum-likelihood phylogeny inferred from the concatenated (supermatrix) dataset of 20 *Microcystis aeruginosa* genes (Table S2). Percentage bootstrap values > 50 % are shown on the branches and based on 1000 replicates using MEGA 11.0.13. The scale bar denotes 0.001 amino acid substitutions per site. The properties of three bicarbonate transporters and toxin stains in 46 *M. aeruginosa* are shown on the right panel. Toxic strains are identified based on the presence of the microcystin (MC) synthase operon, which is consists of the mcyA, B, C, D, E, F, G, H, I, and J genes. Non-toxic strains are the absence of MC. The circles and x indicate present (o) or absence (x) of genes based on the Blast searches. Partial bicA is indicated as /, partial bicA induced by transposon insertion is indicated as /t with the shaded orange box. The midpoint-rooted phylogenetic tree was visualized using the FigTree program (ver.1.4.3).

gene, ccmR2 (LysR-type), is a transcriptional regulator, and the downstream gene, nhaS3, is a sodium/proton antiporter. In the synteny analysis of the bicA–sbtA loci, gene rearrangement was not seen among the 46 genomic strains, but genetic diversity resulted from the partial loss of the bicA gene, full loss of the sbtA gene, or both (Fig. 2). Consequently, we classified six genotypes of the bicA–sbtA loci (Fig. 2 and S2). Half of the 46 genomic strains had the bicA fragment and were categorized as genotypes 4 through 6. Genotypes 4 and 5 included three and two sub-genotypes, respectively. Sub-genotype 4 comprised 18 strains possessing the bicA fragment and sbtA. In sub-genotypes 4–1 through 4–3, various intergenic regions genes were elongated (Fig S2). Intriguingly, Genotype 5 showed an insertion of an IS605 transposon between the partial bicA gene and the sbtA gene (strains *Ma*_NIES-2521, −3787, −3807, and −3804). We found fragments of 314, 662, and 1256 nt of the right end of IS605 (Fig. S2). The 314 and 662 nt derivatives were the results of a one-ended transposition (Bardaji et al., 2011). Genotype 6 included only NIES-88, which had the partial bicA without the three downstream genes, sbtA, sbtB, and nhaS3. Genotypes 2 and 3 had the full-length bicA gene, whereas genotype 3 through 6 have the partial bicA. Interestingly, genotype 3 lacked sbtA/B genes altogether, and these three strains, *Ma*_DIANCHI905, _Sj, and _PCC 7806SL, were potentially toxic strains collected from different geographic locations (Figs. 2, 3 and Table S1). Genotypes 2 retained an intact sbtA gene (1700 nt and 1120 nt in length, respectively), but the intragenic region between sbtB and nhaS3 varied in length between sub-genotypes 2 and 2–1. Genotype 1 possessed a longer bicA fragment due to a 195 nt insertion located at the 5' end (Fig. S2). This insertion was in the middle of the STAT domain and possibly interferes with this gene's function.

The HCO_3^- transporters showed considerable diversity in *M. aeruginosa*. Genetic diversity is accountable for receptivity to environmental influences (Al-Koofee and Mubarak, 2019; Sanjuan and Domingo-Calap, 2016). Therefore, we next analyzed positive selection sites for the HCO_3^- transporters at the genetic level.

3.4. Detection of positive selection sites

To better understand their evolutionary adaptive value, we calculated the position of natural selection sites in HCO_3^- transporter. Positive selection is indicated by accelerated nonsynonymous substitutions and significance is indicated by ω (d_N/d_S) > 1 and p-value < 0.05 (Yang and

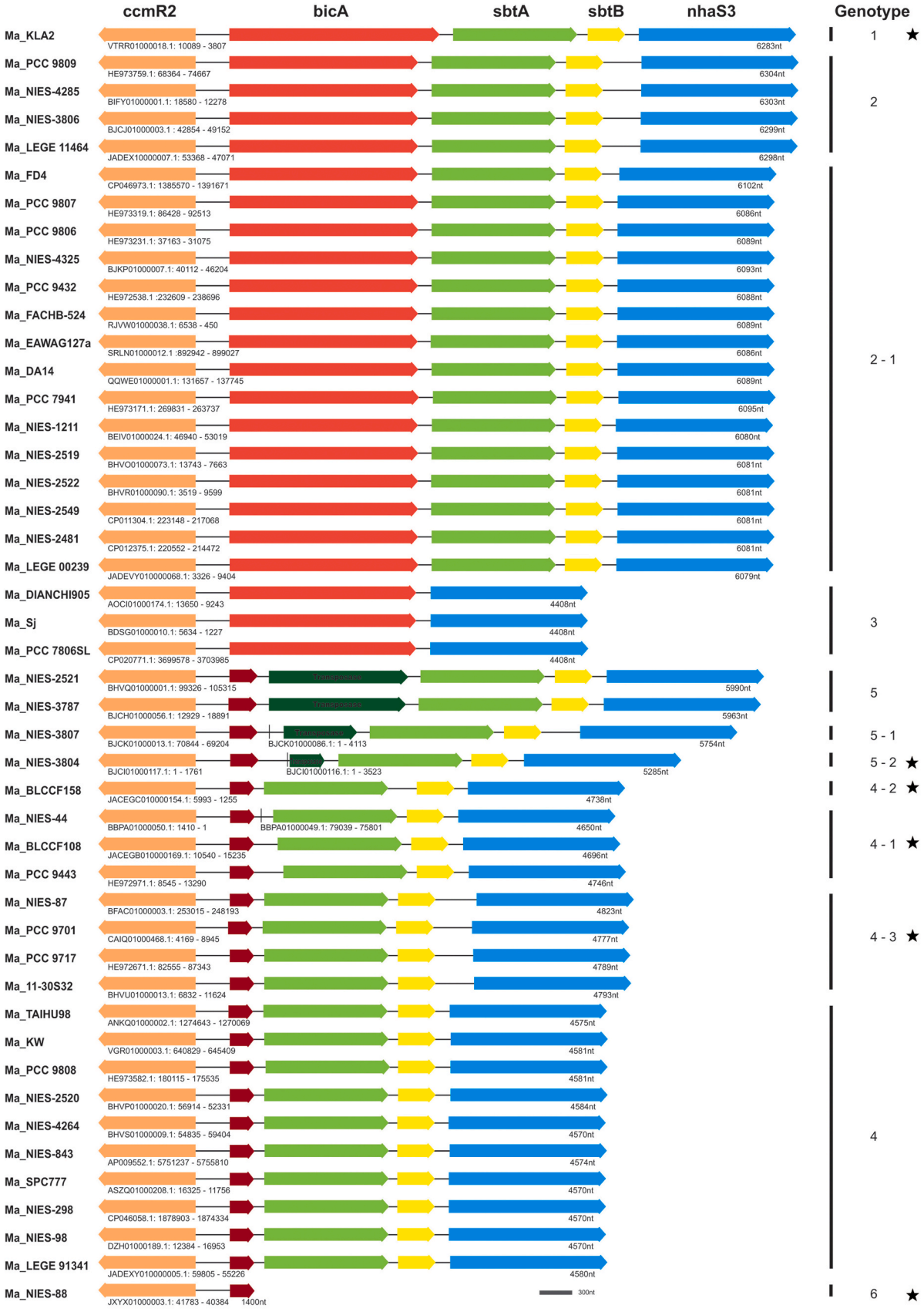

Fig. 2. Synteny of the bicA–sbtA loci from 46 *Microcystis aeruginosa* genomes. The name and loci of scaffold/contig are presented under the synteny bars on the left. Each locus size is shown under the bar on the right. The ccmR2 colored in orange is a transcription regulator. Two bicarbonate transporters, bicA and sbtA, are colored in red (partial gene in dark red) and green, respectively.

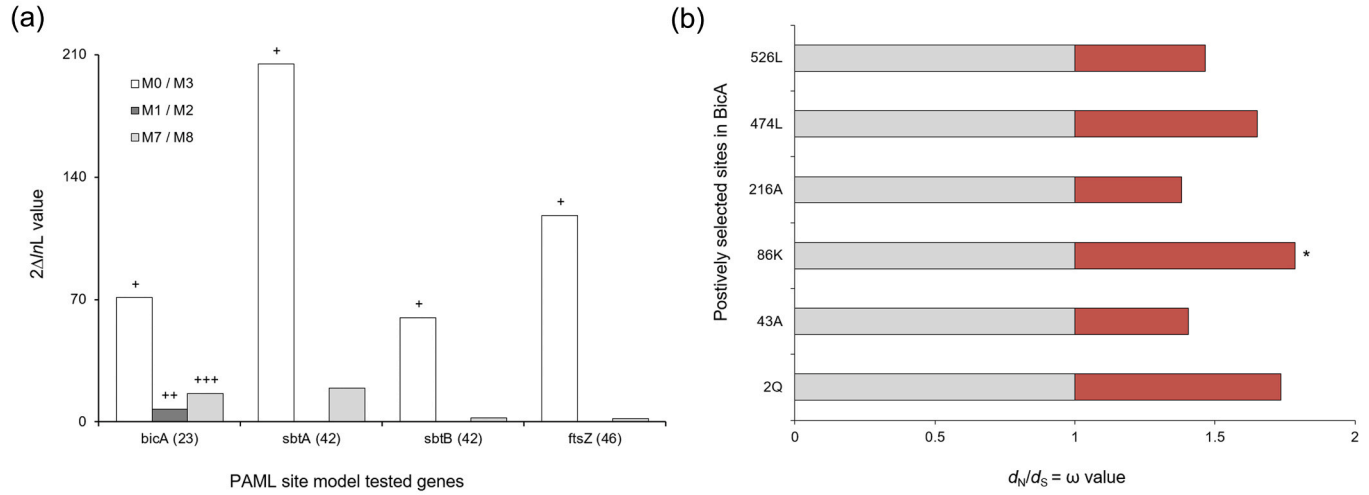

Fig. 3. PAML site modeling and positive Darwinian selection sites of the BicA transporter of *M. aeruginosa*. (a) PAML site model analysis and likelihood ration statistics (+, $p < 0.0001$; ++, $p = 0.02635$; and +++, $p = 0{\cdot}000271$). Numbers in parentheses indicate the number of genes used for PAML analysis. (b) The d_N/d_S (= ω) values of positive selection sites in the BicA transporter of *M. aeruginosa* PCC9807. The six residues shown were predicted to be under positive selection and the asterisk (⁎) indicates a posterior probability of greater than 95 %. Amino acid sequences of positive selection sites showed in Fig. S3.

Reis, 2011). We examined two HCO_3^- transporters, BicA and SbtA, and SbtB (an SbtA regulator) and ftsZ (a housekeeping gene) (Fig. 3a). The analysis using multiple PAML site models showed a significant fit (M3, $\omega = 2.78579$, $p < 0.0001$; M8, $\omega = 2.84459$, $p = 0.00027$) and a marginally significant fit (M2, $\omega = 5.16649$, $p = 0.02635$) for the bicA gene (Fig. 3a and Table S6). The ω values for *Microcystis* BicA were significantly greater than one, indicating a small proportion of relaxed constraints or positive diversifying selection on the gene in natural populations. Six positively selected amino acid sites in the BicA transporter were identified based on Naive Empirical Bayes (NEB) posterior probabilities (Yang and Reis, 2011). These six sites drove adaptive amino acid changes (Fig. 3b). Of the six, four were in the SulP domain (Fig. 4. *Microcystis* PCC9807) and two were in the STAS domain. The STAT domain is at the C-terminus and is responsible for the dimerization of BicA required for bicarbonate ion uptake into cells during the biological transport process (Wang et al., 2019).

3.5. The predicted 2D and 3D structures of BicA

To understand the molecular structure of the *Microcystis* BicA transporter, we predicted its 2D transmembrane topology and 3D homology. In cyanobacterium, the first comprehensive topology of the BicA transporter was analyzed using the pho-lacZ reporter system combined with bioinformatic approaches in *Synechococcus* PCC 7002 (Shelden et al., 2010). In this fusion experiment, the enzyme activity indicated the topological orientation of the construct (Geest and Lolkema, 2000). Initially, cyanobacterial BicA showed 12 full transmembrane regions with intracellular *N*- and *C*-termini. Later, additional transmembrane topology was solved when analyzing the crystal structure of UraA to be used as a modeling template for prestin (Gorbunov et al., 2014). We predicted the topology of *Microcystis* BicA transmembrane topology using the MemBrain (ver. 3.1) web-based program (Fig. 4, showing *Microcystis* PCC9807). The result showed 14 transmembrane (TM) segments with a 7+7 inverted repeat structure, which is consistent with the topologies of related species (Price and Howitt, 2014; Shelden et al., 2010). Furthermore, we investigated the stability of the protein structure by predicting disulfide bond locations. Covalent links between two cysteine residues were located in the TM2 and TM8 regions, respectively (marked by purple diamonds in Fig. 4). This may indirectly support the idea that the substrate-binding pocket consisting of TM3, 8, and 10 has enhanced structural stability (Wang et al., 2019). Further verification is required to confirm the physical function of these disulfide bonds.

The template-based protein structure modeling method can bridge the gap between the number of known sequences and that of 3D models (Fiser, 2010). A previous study has solved the crystal structure of the $BicA^{SulP}$ (PDB: 6KI1) and $BicA^{STAS}$ (PDB: 6KI2) domains from a related cyanobacterium *Synechocystis* sp. PCC6803 (Syn6803) and showed the full-length BicA architecture using a cryo-electron microscopy (cryo--EM) model (Wang et al., 2019). We generated the three-dimensional structure of BicA from *M. aeruginosa* NIES-9807, which was selected as one of the intrinsic strains using homology searching and synteny analysis in this study and which possesses the mcy toxin gene cluster and three bicarbonate transporters (Figs. 2 and 3). In *M. aeruginosa* NIES-9807, the protein sequence identity of the SulP and STAS domains were 68.1 % and 55.4 % when compared with the 6ki1 and 6ki2 templates of *Synechocystis* sp. PCC6803, respectively (data not shown). We tentatively modeled the bicarbonate and sodium ion binding sites based on 6ki1 and 6ki2 as a template and estimated the possible binding positions showing reasonable orientations (Fig. 5b). Substrate-binding pockets were formed by TM3, 8, and 10 in the *Microcystis* BicA transporter consistent with the previous study (Fig. 5c). The substrate-binding sites were highly conserved among the examined cyanobacteria BicA proteins (Fig. 5a). The physical binding sites of the bicarbonate molecule and metal ion and the STAS domain required for BicA activity are reported in a crystal structure study of *Synechocystis* PCC6803 (Wang et al., 2019). This biophysical study showed HCO_3^- and Na_2^+ bound within a hydrophobic pocket formed by TM3, 8, and 10, corroborating our findings here. They have also shown the dimeric structure of the active BicA protein, the binding site of Na_2^+-dependent bicarbonate and the functional mechanism of BicA in cell physiology and carbon assimilation (Wang et al., 2019). Integrating our in-silico analysis results, the *Microcystis* BicA transporter had well-conserved substrate binding sites that is tightly connected to TM2 and TM8 by the covalent link. This transporter thus appears to be functionally well conserved, though this requires further molecular verification.

4. Discussion

Dramatic changes in pH and nutrient supply in freshwater alter carbon acquisition, shifting inorganic carbon chemistry toward HCO_3^- under conditions of high photosynthesis and alkaline pH (Badger et al., 2006; Mokashi et al., 2016). The very dense *Microcystis* blooms can decrease the HCO_3^- concentration and increase pH to >10, shifting the

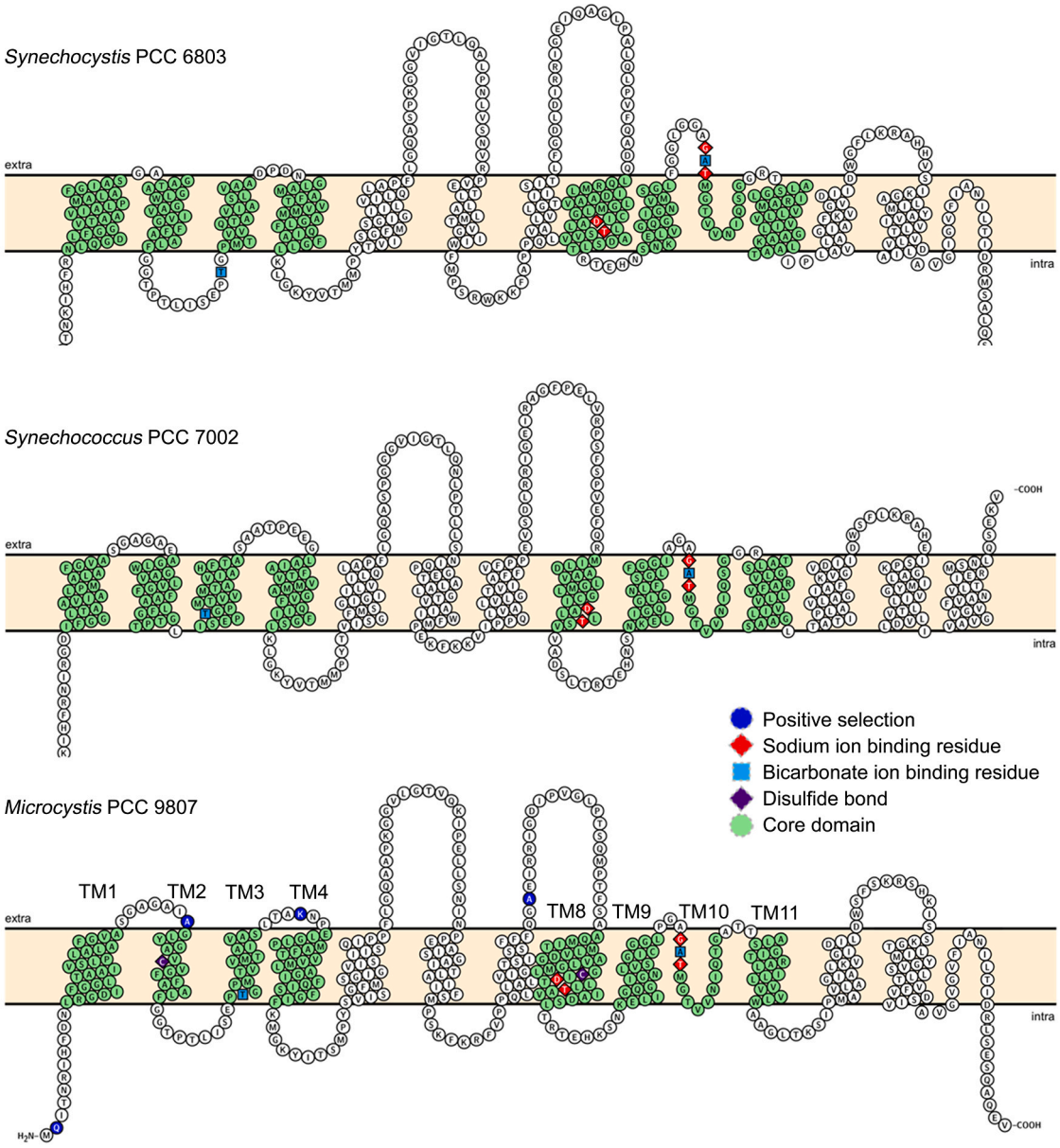

Fig. 4. Transmembrane (TM) topology of the BicA transporter of *Microcystis* PCC 9807. A consensus topology of *Microcystis aeruginosa* BicA transporter (bottom topology) shows only the SulP domain with a 7+7 inverted repeat structure. The BicA protein consists of core domains (light green color) and gate domains (white color). The topologies of *Synechocystis* PCC6803 (Q55415) and *Synechococcus* PCC7002 (Q14SY0) were experimentally confirmed TM regions. Both protein sequences were retrieved from uniprot at https://www.uniprot.or. The visualization was produced using the Protter web-based program.

balance from HCO_3^- to CO_3^{2-} as the dominant inorganic carbon species (Ji et al., 2020). *Microcystis* growth potentially influence the carbon cycle within the blooms. Conversely, it may also impact the diversity of genes encoding bicarbonate transporters, allowing adaptation to fluctuating carbon sources. Therefore, this study employed computational approaches to explore the potential ecological significance of HCO_3^- transporters in *M. aeruginosa*. Phylogeny analysis revealed extensive distribution of both partial and full-length bicA gene worldwide (Fig. 1 and Table S1). It suggests that the bicA gene initially experienced significant sequence loss before spreading globally, indicating the potential for local reselection of stains containing the full-length of bicA gene (Fig. 1). Intriguingly, among the four strains (*Ma*_NIES-2521, −3787, −3807, and −3804), the partial bicA fragment had been truncated by IS605 derivatives of varying lengths (Fig. 2). It is noteworthy that all four strains were collected from Lake Kasumigaura in Japan and were reported in the same year (Table S1). This finding raises the question of whether transposon IS605 will eventually disappear or whether miniature IS605 selectively targets the bicA gene (Bardaji et al., 2011). Another transposon, ISMae4, also divides the bicA gene into two fragments (Sandrini et al., 2014). Interestingly, both transposons silenced the bicA gene, leading to its genetic and structural diversity in *M. aeruginosa*. The research on the silencing of target genes by these transposable elements still remains unknown. Additionally, we investigated 11 strains with partial bicA originating from Lake Kamugra, Japan, including the aforementioned four strains. This alignment of the loss sequences revealed consistency between the four strains with partial bicA and transposon insertion as well as the other strains–NIES_44, _88, _843, and 284 (Fig. 6). Fascinatingly, the terminal sequencing of the strain with the transposon inserted and other partial bicA strains were conserved, thought the conserved sequences differed (Fig. 6. the bottom). This result suggested that the conserved terminal sequences was remnants of the deletion. Gene loss events and genetic variants can serve

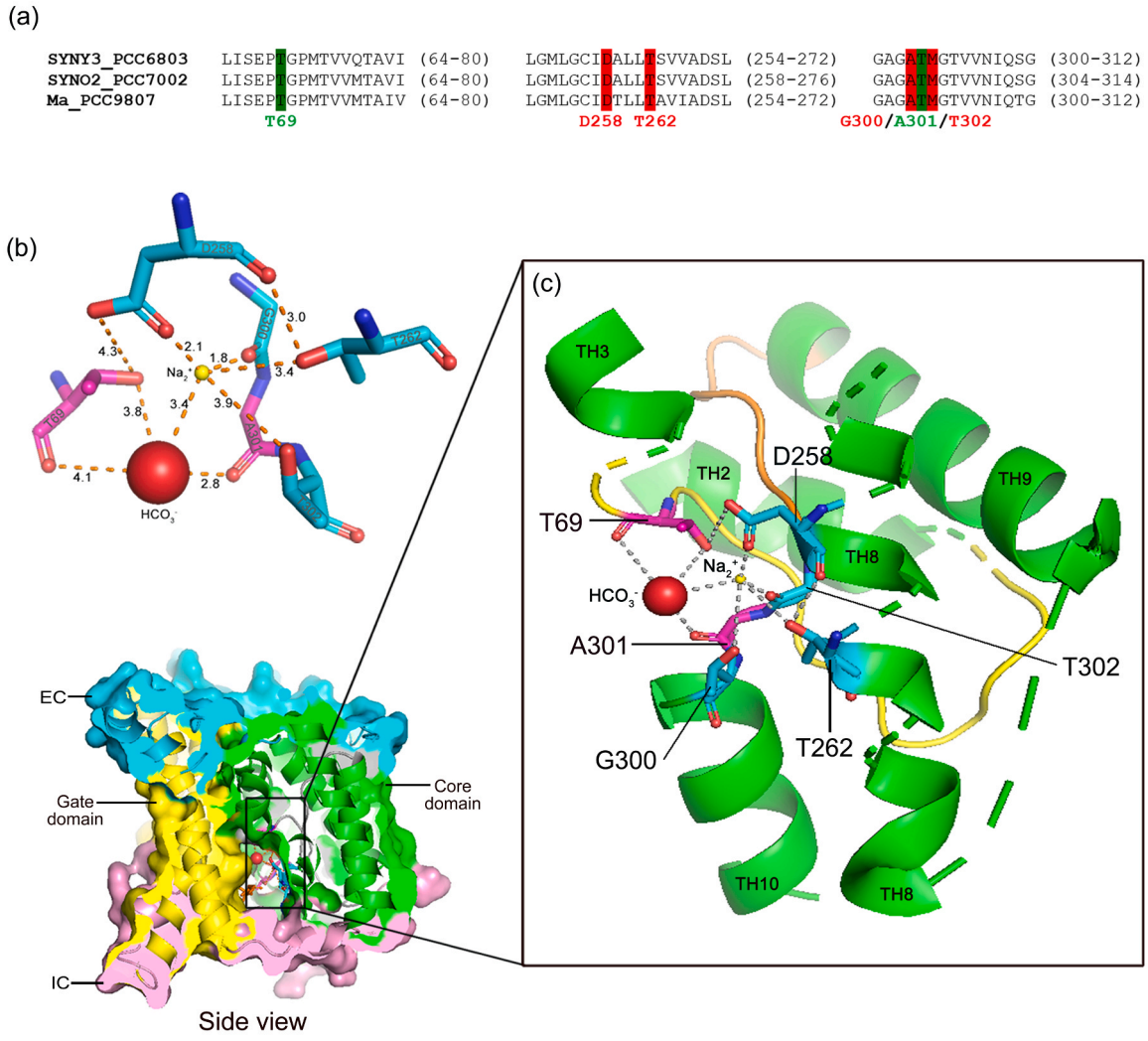

Fig. 5. The 3D homology modeling for the *Microcystis aeruginosa* BicA transporter. (a) The conserved ion binding motifs (Wang et al., 2019). The binding sites of the sodium and bicarbonate ion are marked by green and red boxes, respectively (b) The tentatively estimated distances between the substrate-binding sites and bicarbonate and sodium ions, which are represented by circular spheres colored in red and yellow, respectively. (c) The magnified box shows the binding residues of the bicarbonate and sodium ions colored in pink and sky blue, respectively. Gate domain, Core domain, EC (extracellular), and IC (intracellular) are colored yellow, green, light sky blue, and pink, respectively.

as indicators of adaptive functions. This observation provides insights into whether positive or negative selection occurred in response to environmental interactions (Bourque et al., 2018; Meyer et al., 2017) and it is of significant interest from both an ecological and evolutionary perspectives. Collectively, these results highlight the importance of strain-specific characterization in understanding *Microcystis* blooms.

In addition to the loss event of the bicA gene, the statistical values of the PAML site models significantly showed the occurrence of positive selection on the *Microcystis* bicA gene (Fig. 3). The main assertion of the d_N/d_S ratio (= ω) is that random fixation of alleles causes most observed interspecific genetic diversity (Derbyshire, 2020). The positive selections at Ala43, Lys86, and Val216 of BicA occurred at the surface of the extracellular membrane, a favorable location for encountering intracellular ions (Fig. 4). The BicA transporter binds to its substrate (Na^+/HCO_3^-) with relatively low affinity, meaning it require higher substrate levels to function effectively compared to SbtA, which has high affinity. The occurrence of positive sites in BicA, but not in SbtA and SbtB (Fig. 3a), does not preclude the possibility of genetic selection. However, it is unclear whether these selective advantages are in response to carbon pressures in this study.

Cyanobacterial CCMs exhibit cellular structural and phylogenetic differences when compared to the majority of CCMs found in eukaryotic microalgae (Renberg et al., 2010). Cyanobacteria have only thylakoid membranes in the cytoplasm and carboxysomes that concentrate CO_2 around RuBisCO. In contrast, eukaryotic microalgae have pyrenoids, which are membrane-bound organelles located in their chloroplasts (Mario Giordano and Raven, 2005). Thus, cyanobacterial CCM is energy-efficient and does not require multiple HCO_3^- transporters (Rottet et al., 2021). In evolutionary origins, eukaryotic microalgae evolved later, acquiring photosynthesis through endosymbiosis with cyanobacteria-like ancestors (Goudet et al., 2020; Kupriyanova et al., 2013).Despite differences in cellular structure and evolutionary origin, previous studies have shown an increase in the high CO_2 uptake rate of *Microcystis* at elevated *p*CO2, similar to that reported for green microalgae (Ji et al., 2020).

Recent molecular and biochemical investigations have shed light on the BicA and SbtA transporter systems in cyanobacteria (Fang et al., 2021; Kaczmarski et al., 2019). Bicarbonate transporters of the SLC26 and SLC4 families in cyanobacteria have provided valuable insights into how these organisms absorb HCO_3^- to regulate their internal pH and perform photosynthesis (Wang et al., 2019). Structural studies have revealed a variety of substrates and their binding sites. Human SLC4A1 and SLC26A3 function as Cl^--coupled HCO_3^- transporter, whereas human SLC4A4 and three microalgal BicA are Na^+-coupled HCO_3^- transporters.

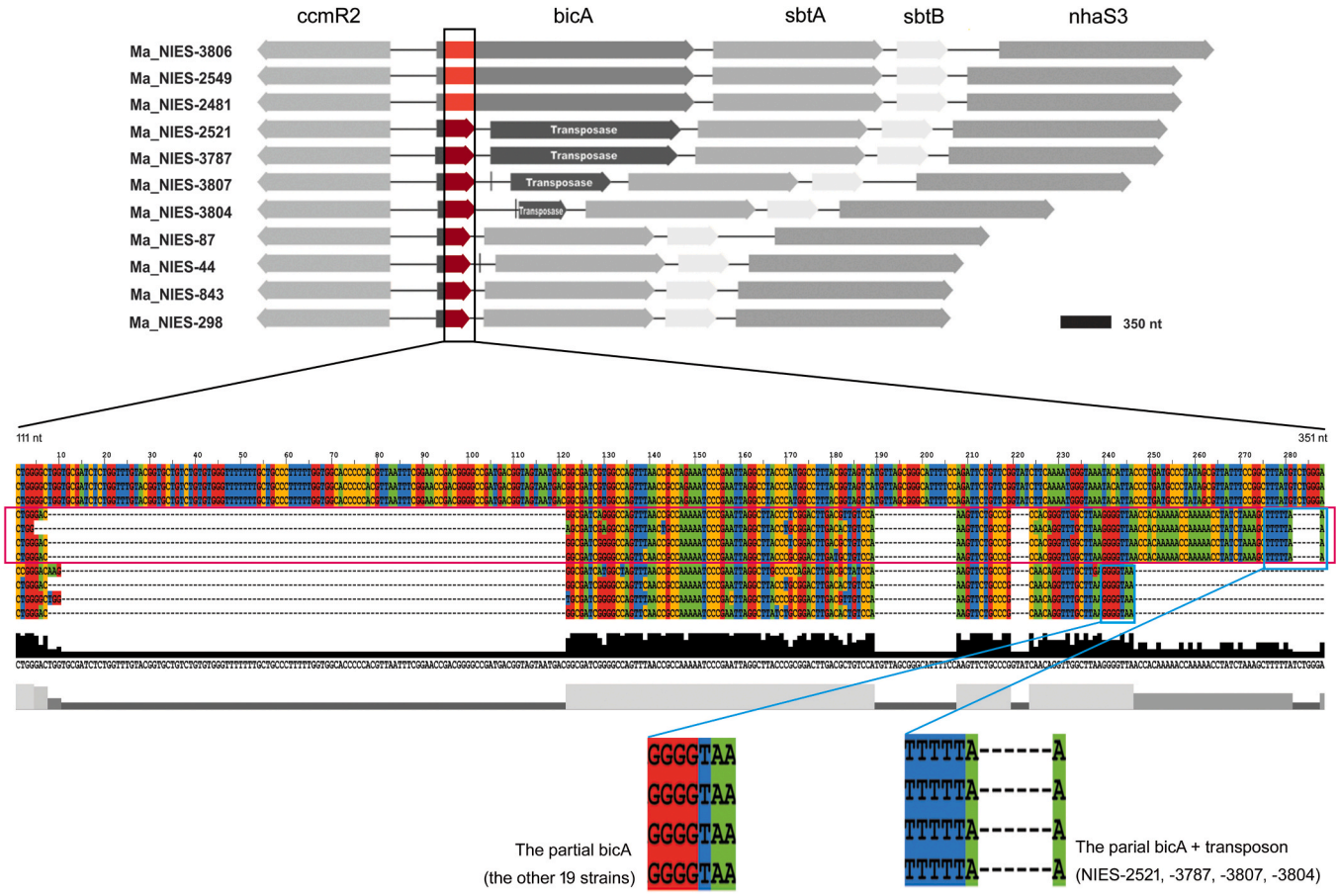

Fig. 6. The alignment of full and partial bicA sequences from Lake Kasumigaura, Japan. The selected 11 strains were originated from the same lake. Three strains (NIES-3806, −2549, −2481) possess the full sequence of bicA, while the others have partial bicA sequences. The pink box indicates stains with the partial bicA and transposon insertions. The light blue color of two boxes indicates the terminal sequence for each group. The alignment was performed using MAFFT at mafft.cbrc.jp/alignment/server/.

In *Microcystis* BicA, we confirmed that HCO_3^- interacts with four sites, including the carbonyl group of Thr69 and Asp301, as well as the metal ion. A structure-based analysis reveals that the T-loop of SbtB controls the activity of SbtA, by immobilizing it in an inward-facing state during illumination/darkness cycles. Otherwise, the study of BicA explores the specific amino acid residues for binding HCO_3^- ions, discussing how efficient HCO_3^- transporters contribute to enable cyanobacteria to thrive in carbon-limited environments. In cyanobacteria, molecular structural analysis has provided evidence of the molecular physics of Na_2^+-dependent HCO_3^- ion transport into cells. In this study, we predicted the topology and three-dimensional modeling of *Microcystis* BicA transporter. These results showed a high degree of structural conservation in *Microcystis* BicA transporter, characterized by the presence of residues binding to both sodium and bicarbonate ions. This suggests functional conservation within the transporter.

The species *M. aeruginosa* often thrive in environments where conditions fluctuate depending on the availability of carbon sources. Typically, genes for proteins annotated as functions of CCM and defined enzymatic steps in the central C metabolisms are differentially expressed in wild type cells under different Ci conditions. Also, each transporter possesses a distinct carbon binding affinity, and specific genes will selectively respond to varying carbon conditions (Kupriyanova et al., 2013; Raven et al., 2012). However, research on the ecological functions of active bicarbonate transporters within various strain-level combinations in the species *M. aeruginosa* remains incomplete. The expression of the HCO_3^- transporter genes show considerable diversity depending on the species or environmental conditions. In laboratory cultures of *M. aeruginosa*, the bicA and sbtA genes exhibit relatively higher expression at the surface, whereas BCT1 is constitutively expressed both at the surface and bottom (Srivastava et al., 2019). It is assumed that the surface water in the flask contains better light, oxygen, and carbon dioxide, providing favorable conditions for algae growth. For bloom studies, this laboratory experiment imply that column-sectional carbon depletion or repletion models could demonstrate the ecological functions of bicarbonate transports when thermal stratification in freshwater. In addition, the protein abundance of *Microcystis* BCT1 is consistent with its gene expression, showing notably lower in comparison to those of the bicA and sbtA genes (Fig. S4). Furthermore, the duration of exposure to the CO_2 limited condition affect the expression of the bicA gene. In *Cyanothece*, bicA expression increases after 24 hours under carbon depletion (Kupriyanova et al., 2019). Conversely, in *Synechocystis*, bicA expression increases slightly up to 3 hours but decreases after 24 hours of exposure (Eisenhut et al., 2007). Besides species differences, the duration of exposure to CO_2 limitation also influences the dynamic expression of the bicA gene.

Finally, understanding how various strains utilize bicarbonate informs strategies for managing nutrients to prevent bloom formation. Studying the ecological roles of bicarbonate transporters in carbon fluxes offers insights for directing water conservation efforts. Enhancing bicarbonate transporter in genetically modified cyanobacteria could improve carbon sequestration or biofuel production in bioreactors. These examples demonstrate how integrating ecological and genetic research on cyanobacterial carbon acquisition can contribute to advancements in biotechnology, ecosystems health, climate change

mitigation and environmental management.

5. Conclusion

Our current findings have constraints in elucidating the global preference for the reselection of the bicA gene after experiencing partial deletion caused by the IS605 transposon, as well as the reasons behind the positive selection observed in the bicA gene. However, we have presented evidence highlighting the significance of the *Microcystis* BicA transporter in its role in carbon uptake, particularly during periods of carbon starvation or the occurrence of cyanobacterial blooms. To expand our comprehension of the ecological role of the bicA gene as a transporter of photosynthetic carbon during the blooms, we suggest investigating the ecological phenomena specific to each region by utilizing strains from those respective regions. Understanding this information will be crucial for exploring intraspecific competition, especially in determining whether a particular strain with the bicA gene contributes to enhanced biomass under specific conditions. Conducting comparative studies that integrate ecological data with molecular experiments is imperative.

CRediT authorship contribution statement

Seong-il Eyun: Writing – review & editing, Writing – original draft, Formal analysis, Data curation, Conceptualization. **Jihye Yang:** Formal analysis. **Huijeong Doh:** Formal analysis. **Eun-Jeong Kim:** Writing – review & editing, Writing – original draft, Formal analysis, Conceptualization.

Declaration of Competing Interest

The authors declare that they have no known competing financial interests or personal relationships that could have appeared to influence the work reported in this paper.

Data availability

Data will be made available on request.

Acknowledgements

This work was supported by the National Research Foundation of Korea grants (2022R1A2C4002058), Korea Institute of Marine Science & Technology Promotion (KIMST) funded by the Ministry of Oceans and Fisheries (RS-2022-KS221676), and the Chung-Ang University Graduate Research Scholarship in 2023.

Appendix A. Supporting information

Supplementary data associated with this article can be found in the online version at doi:10.1016/j.ecoenv.2024.116795.

References

Al-Koofee, D.A.F., Mubarak, S.M.H., 2019. Genetic Polymorphisms, The Recent Topics in Genetic Polymorphisms. IntechOpen.

Badger, M.R., Price, G.D., Long, B.M., Woodger, F.J., 2006. The environmental plasticity and ecological genomics of the cyanobacterial CO_2 concentrating mechanism. J. Exp. Bot. 57, 249–265.

Ban, N., Beckmann, R., Cate, J.H., Dinman, J.D., Dragon, F., Ellis, S.R., Lafontaine, D.L., Lindahl, L., Liljas, A., Lipton, J.M., McAlear, M.A., Moore, P.B., Noller, H.F., Ortega, J., Panse, V.G., Ramakrishnan, V., Spahn, C.M., Steitz, T.A., Tchorzewski, M., Tollervey, D., Warren, A.J., Williamson, J.R., Wilson, D., Yonath, A., Yusupov, M., 2014. A new system for naming ribosomal proteins. Curr. Opin. Struct. Biol. 24, 165–169.

Bardaji, L., Anorga, M., Jackson, R.W., Martinez-Bilbao, A., Yanguas-Casas, N., Murillo, J., 2011. Miniature transposable sequences are frequently mobilized in the bacterial plant pathogen Pseudomonas syringae pv. phaseolicola. PLoS One 6, e25773.

Battchikova, N., Vainonen, J.P.V., Natalia Keränen, Mika, Carmel, D., Aro, E.-M., 2010. Dynamic changes in the proteome of synechocystis 6803 in response to CO_2 limitation revealed by quantitative proteomics. J. Proteome Res. 9, 5896–5912.

Berry, M.A., Davis, T.W., Cory, R.M., Duhaime, M.B., Johengen, T.H., Kling, G.W., Marino, J.A., Den Uyl, P.A., Gossiaux, D., Dick, G.J., Denef, V.J., 2017. Cyanobacterial harmful algal blooms are a biological disturbance to Western Lake Erie bacterial communities. Environ. Microbiol 19, 1149–1162.

Bourque, G., Burns, K.H., Gehring, M., Gorbunova, V., Seluanov, A., Hammell, M., Imbeault, M., Izsvak, Z., Levin, H.L., Macfarlan, T.S., Mager, D.L., Feschotte, C., 2018. Ten things you should know about transposable elements. Genome Biol. 19, 199.

Derbyshire, M.C., 2020. Bioinformatic detection of positive selection pressure in plant pathogens: the neutral theory of molecular sequence evolution in action. Front. Microbiol 11, 644.

Dick, G.J., Duhaime, M.B., Evans, J.T., Errera, R.M., Godwin, C.M., Kharbush, J.J., Nitschky, H.S., Powers, M.A., Vanderploeg, H.A., Schmidt, K.C., Smith, D.J., Yancey, C.E., Zwiers, C.C., Denef, V.J., 2021. The genetic and ecophysiological diversity of Microcystis. Environ. Microbiol.

Eisenhut, M., Aguirre von Wobeser, E., Jonas, L., Schubert, H., Ibelings, B.W., Bauwe, H., Matthijs, H.C., Hagemann, M., 2007. Long-term response toward inorganic carbon limitation in wild type and glycolate turnover mutants of the cyanobacterium Synechocystis sp. strain PCC 6803. Plant Physiol. 144, 1946–1959.

Eyun, S., 2019. Accelerated pseudogenization of trace amine-associated receptor genes in primates. Genes Brain Behav. 18, e12543.

Fang, S., Huang, X., Zhang, X., Zhang, M., Hao, Y., Guo, H., Liu, L.-N., Yu, F., Zhang, P., 2021. Molecular mechanism underlying transport and allosteric inhibition of bicarbonate transporter SbtA. Proc. Natl. Acad. Sci. USA 118, e2101632118.

Fiser, A., 2010. Template-based protein structure modeling. Methods Mol. Biol. 673, 73–94.

Gaudana, S.B., Zarzycki, J., Moparthi, V.K., Kerfeld, C.A., 2015. Bioinformatic analysis of the distribution of inorganic carbon transporters and prospective targets for bioengineering to increase Ci uptake by cyanobacteria. Photosynth Res. 126, 99–109.

Geest, M.V., Lolkema, J.S., 2000. Membrane TOpology and Insertion of Membrane Proteins: Search for Topogenic Signals. Microbiol. Mol. Biol. Rev. 64, 21.

Gorbunov, D., Sturlese, M., Nies, F., Kluge, M., Bellanda, M., Battistutta, R., Oliver, D., 2014. Molecular architecture and the structural basis for anion interaction in prestin and SLC26 transporters. Nat. Commun. 5, 3622.

Goudet, M.M.M., Orr, D.J., Melkonian, M., Müller, K.H., Meyer, M.T., Carmo-Silva, E., Griffiths, H., 2020. Rubisco and carbon-concentrating mechanism co-evolution across chlorophyte and streptophyte green algae. New Phytol. 227, 810–823.

Griffith, A.W., Gobler, C.J., 2020. Harmful algal blooms: a climate change co-stressor in marine and freshwater ecosystems. Harmful Algae 91, 101590.

Harke, M.J., Gobler, C.J., 2015. Daily transcriptome changes reveal the role of nitrogen in controlling microcystin synthesis and nutrient transport in the toxic cyanobacterium, Microcystis aeruginosa. BMC Genom. 16, 1068.

Herrero, A., Flores, E., 2019. Genetic responses to carbon and nitrogen availability in Anabaena. Environ. Microbiol. 21, 1–17.

Jeon, M.S., Jeong, D.M., Doh, H., Kang, H.A., Jung, H., Eyun, S., 2023. A practical comparison of the next-generation sequencing platform and assemblers using yeast genome. Life Sci. Alliance 6 e202201744.

Ji, X., Verspagen, J.M.H., Stomp, M., Huisman, J., 2017. Competition between cyanobacteria and green algae at low versus elevated CO2: who will win, and why? J. Exp. Bot. 68, 3815–3828.

Ji, X., Verspagen, J.M.H., Waal, D.B.Vd, Rost, B., Huisman, J., 2020. Phenotypic plasticity of carbon fixation stimulates cyanobacterial blooms at elevated CO_2. Sci. Adv. 6, eaax2926.

Jung, H., Ventura, T., Chung, J.S., Kim, W.-J., Nam, B.-H., Kong, H.J., Kim, Y.-O., Jeon, M.-S., Eyun, S.-i, 2020. Twelve quick steps for genome assembly and annotation in the classroom. PLoS Comput. Biol. 16, e1008325.

Kaczmarski, J.A., Hong, N.S., Mukherjee, B., Wey, L.T., Rourke, L., Forster, B., Peat, T.S., Price, G.D., Jackson, C.J., 2019. Structural basis for the allosteric regulation of the SbtA Bicarbonate Transporter by the PII-like Protein, SbtB, from cyanobium sp. PCC7001. Biochemistry 58, 5030–5039.

Kaneko, T., Nakajima, N., Okamoto, S., Suzuki, I., Tanabe, Y., Tamaoki, M., Nakamura, Y., Kasai, F., Watanabe, A., Kawashima, K., Kishida, Y., Ono, A., Shimizu, Y., Takahashi, C., Minami, C., Fujishiro, T., Kohara, M., Katoh, M., Nakazaki, N., Nakayama, S., Yamada, M., Tabata, S., Watanabe, M.M., 2007. Complete genomic structure of the bloom-forming toxic cyanobacterium Microcystis aeruginosa NIES-843. DNA Res.: Int. J. Rapid Publ. Rep. Genes Genomes 14, 247–256.

Katoh, K., Standley, D.M., 2013. MAFFT multiple sequence alignment software version 7: improvements in performance and usability. Mol. Biol. Evol. 30, 772–780.

Kupriyanova, E.V., Sinetova, M.A., Cho, S.M., Park, Y.I., Los, D.A., Pronina, N.A., 2013. CO_2-concentrating mechanism in cyanobacterial photosynthesis: organization, physiological role, and evolutionary origin. Photosynth. Res. 117, 133–146.

Kupriyanova, E.V., Sinetova, M.A., Mironov, K.S., Novikova, G.V., Dykman, L.A., Rodionova, M.V., Gabrielyan, D.A., Los, D.A., 2019. Highly active extracellular alpha-class carbonic anhydrase of Cyanothece sp. ATCC 51142. Biochimie 160, 200–209.

Li, Q., Lin, F., Yang, C., Wang, J., Lin, Y., Shen, M., Park, M.S., Li, T., Zhao, J., 2018. A large-scale comparative metagenomic study reveals the functional interactions in six bloom-forming microcystis-epibiont communities. Front. Microbiol. 9, 746.

Mario Giordano, J.B., Raven, John A., 2005. CO2 concentrating mechanisms in algae: mechanisms, environmental modulation, and evolution. Annu. Rev. Plant Biol. 56, 99–131.

Meyer, K.A., Davis, T.W., Watson, S.B., Denef, V.J., Berry, M.A., Dick, G.J., 2017. Genome sequences of lower Great Lakes Microcystis sp. reveal strain-specific genes that are present and expressed in western Lake Erie blooms. PLoS One 12, e0183859.
Mokashi, K., Shetty, V., George, S.A., Sibi, G., 2016. Sodium Bicarbonate as Inorganic Carbon Source for Higher Biomass and Lipid Production Integrated Carbon Capture in Chlorella vulgaris. Achiev. Life Sci. 10, 111–117.
Okano, K., Miyata, N., Ozaki, Y., 2015. Whole Genome Sequence of the Non-Microcystin-Producing Microcystis aeruginosa Strain NIES-44. Genome Announc. 3 e00135-00115.
Price, G.D., 2011. Inorganic carbon transporters of the cyanobacterial CO_2 concentrating mechanism. Photosynth. Res. 109, 47–57.
Price, G.D., Howitt, S.M., 2014. Topology mapping to characterize cyanobacterial bicarbonate transporters: BicA (SulP/SLC26 family) and SbtA. Mol. Membr. Biol. 31, 177–182.
Price, G.D., Shelden, M.C., Howitt, S.M., 2011. Membrane topology of the cyanobacterial bicarbonate transporter, SbtA, and identification of potential regulatory loops. Mol. Membr. Biol. 28, 265–275.
Price, G.D., Woodger, F.J., Badger, M.R., Howitt, S.M., Tucker, L., 2004. Identification of a SulP-type bicarbonate transporter in marine cyanobacteria. PNAS 101.
Rantala, A., Fewer, D.P., Hisbergues, M., Rouhiainen, L., Vaitomaa, J., Borner, T., Sivonen, K., 2004. Phylogenetic evidence for the early evolution of microcystin synthesis. Proc. Natl. Acad. Sci. USA 101, 568–573.
Raven, J.A., Giordano, M., Beardall, J., Maberly, S.C., 2012. Algal evolution in relation to atmospheric CO_2: carboxylases, carbon-concentrating mechanisms and carbon oxidation cycles. Philos. Trans. R. Soc. Lond. B Biol. Sci. 367, 493–507.
Reinhold, A.Ka.L., 1999. CO_2 concentrating mechanisms in photosynthetic microorganisms. Annu. Rev. Plant Physiol. Plant Mol. Biol. 50, 539–570.
Renberg, L., Johansson, A.I., Shutova, T., Stenlund, H., Aksmann, A., Raven, J.A., Gardestrom, P., Moritz, T., Samuelsson, G., 2010. A metabolomic approach to study major metabolite changes during acclimation to limiting CO_2 in Chlamydomonas reinhardtii. Plant Physiol. 154, 187–196.
Rolland, V., Badger, M.R., Price, G.D., 2016. Redirecting the cyanobacterial bicarbonate transporters BicA and SbtA to the chloroplast Envelope: soluble and membrane cargos need different chloroplast targeting signals in plants. Front. Plant Sci. 7, 185.
Rottet, S., Forster, B., Hee, W.Y., Rourke, L.M., Price, G.D., Long, B.M., 2021. Engineered accumulation of bicarbonate in plant chloroplasts: known knowns and known unknowns. Front. Plant Sci. 12, 727118.
Sandrini, G., Ji, X., Verspagen, J.M., Tann, R.P., Slot, P.C., Luimstra, V.M., Schuurmans, J.M., Matthijs, H.C., Huisman, J., 2016. Rapid adaptation of harmful cyanobacteria to rising CO_2. Proc. Natl. Acad. Sci. USA 113, 9315–9320.
Sandrini, G., Matthijs, H.C.P., Verspagen, J.M.H., Muyzer, G., Huisman, J., 2014. Genetic diversity of inorganic carbon uptake systems causes variation in CO_2 response of the cyanobacterium Microcystis. ISME J. 8, 589–600.
Sanjuan, R., Domingo-Calap, P., 2016. Mechanisms of viral mutation. Cell Mol. Life Sci. 73, 4433–4448.
Shelden, M.C., Howitt, S.M., Price, G.D., 2010. Membrane topology of the cyanobacterial bicarbonate transporter, BicA, a member of the SulP (SLC26A) family. Mol. Membr. Biol. 27, 12–22.
Shibata, M.O., Hiroshi, Katoh, H., Shimoyama, M., OgawaA, T., 2002. Two CO_2 uptake systems in cyanobacteria: four systems for inorganic carbon acquisition in Synechocystis sp. strain PCC6803. Funct. Plant Biol. 29, 123–129.
Smith, R.B., Bass, B., Sawyer, D., Depew, D., Watson, S.B., 2019. Estimating the economic costs of algal blooms in the Canadian Lake Erie Basin. Harmful Algae 87, 101624.
Srivastava, A., Jeong, H., Ko, S.-R., Ahn, C.-Y., Choi, J.W., Park, Y.I., Neilan, B.A., Oh, H.-M., 2019. Phenotypic niche partitioning and transcriptional responses of Microcystis aeruginosa in a spatially heterogeneous environment. Algal Res. 41, 101551.
Sun, L.W., Jiang, W.J., Sato, H., Kawachi, M., Lu, X.W., 2016. Rapid classification and identification of microcystis aeruginosa strains using MALDI-TOF MS and polygenetic analysis. PLoS One 11, e0156275.
Tamura, K., Stecher, G., Kumar, S., 2021. MEGA11: molecular evolutionary genetics analysis version 11. Mol. Biol. Evol. 38, 3022–3027.
Tanabe, Y., Hodoki, Y., Sano, T., Tada, K., Watanabe, M.M., 2018. Adaptation of the freshwater bloom-forming cyanobacterium microcystis aeruginosa to brackish water is driven by recent horizontal transfer of sucrose genes. Front. Microbiol. 9, 1150.
Tanabe, Y., Kasai, F., Watanabe, M.M., 2007. Multilocus sequence typing (MLST) reveals high genetic diversity and clonal population structure of the toxic cyanobacterium Microcystis aeruginosa. Microbiology 153, 3695–3703.
Tang, J., Zhou, H., Yao, D., Riaz, S., You, D., Klepacz-Smolka, A., Daroch, M., 2022. Comparative genomic analysis revealed distinct molecular components and organization of CO_2-concentrating mechanism in thermophilic cyanobacteria. Front Microbiol 13, 876272.
Wang, Sun, B., Zhang, X., Huang, X., Zhang, M., Guo, H., Chen, X., Huang, F., Chen, T., Mi, H., Yu, F., Liu, L.N., Zhang, P., 2019. Structural mechanism of the active bicarbonate transporter from cyanobacteria. Nat. Plants 5, 1184–1193.
Wang, S., Zhang, X., Wang, C., Chen, N., 2023. Temporal continuous monitoring of cyanobacterial blooms in Lake Taihu at an hourly scale using machine learning. Sci. Total Environ. 857, 159480.
Yang, Z., Reis, Md, 2011. Statistical properties of the branch-site test of positive selection. Mol. Biol. Evol. 28, 1217–1228.
Yuan, R., Li, J., Li, Y., Ren, L., Wang, S., Kong, F., 2019. Formation mechanism of the Microcystis aeruginosa bloom in the water with low dissolved phosphorus. Mar. Pollut. Bull. 148, 194–201.
Zhang, J., Nielsen, R., Yang, Z., 2005. Evaluation of an improved branch-site likelihood method for detecting positive selection at the molecular level. Mol. Biol. Evol. 22, 2472–2479.
Zhou, Y., Zhang, X., Li, X., Jia, P., Dai, R., 2019. Evaluation of changes in Microcystis aeruginosa growth and microcystin production by urea via transcriptomic surveys. Sci. Total Environ. 655, 181–187.